Received: 5 June 2024 | Revised: 7 August 2024 | Accepted: 17 September 2024

DOI: 10.1002/jor.25984

Journal of Orthopaedic Research®

RESEARCH ARTICLE

How accurately do finite element models predict the fall impact response of ex vivo specimens augmented by prophylactic intramedullary nailing?

Emily K. Bliven[1] | Anita Fung[2] | Alexander Baker[2] | Ingmar Fleps[3] | Stephen J. Ferguson[2] | Pierre Guy[4,5] | Benedikt Helgason[2] | Peter A. Cripton[1,5]

[1]School of Biomedical Engineering, University of British Columbia, Vancouver, British Columbia, Canada

[2]Institute for Biomechanics, ETH Zürich, Zürich, Switzerland

[3]Skeletal Mechanobiology & Biomechanics Laboratory, Department of Mechanical Engineering, Boston University, Boston, Massachusetts, USA

[4]Division of Orthopaedic Trauma, Department of Orthopaedics, University of British Columbia, Vancouver, British Columbia, Canada

[5]Centre for Aging SMART, University of British Columbia, Vancouver, British Columbia, Canada

Correspondence

Anita Fung, Institute for Biomechanics, ETH Zürich, Zürich, Switzerland.
Email: anita.fung@hest.ethz.ch

Funding information

Faculty of Medicine, University of British Columbia, Grant/Award Number: Friedman Award for Scholars in Health; Eidgenössische Technische Hochschule Zürich, Grant/Award Number: #2018-430; Schweizerischer Nationalfonds zur Förderung der Wissenschaftlichen Forschung, Grant/Award Number: 205320_169331

Abstract

Hip fracture prevention approaches like prophylactic augmentation devices have been proposed to strengthen the femur and prevent hip fracture in a fall scenario. The aim of this study was to validate the finite element model (FEM) of specimens augmented by prophylactic intramedullary nailing in a simulated sideways fall impact against ex vivo experimental data. A dynamic inertia-driven sideways fall simulator was used to test six cadaveric specimens (3 females, 3 males, age 63–83 years) prophylactically implanted with an intramedullary nailing system used to augment the femur. Impact force measurements, pelvic deformation, effective pelvic stiffness, and fracture outcomes were compared between the ex vivo experiments and the FEMs. The FEMs over-predicted the effective pelvic stiffness for most specimens and showed variability in terms of under- and over-predicting peak impact force and pelvis compression depending on the specimen. A significant correlation was found for time to peak impact force when comparing ex vivo and FEM data. No femoral fractures were found in the ex vivo experiments, but two specimens sustained pelvic fractures. These two pelvis fractures were correctly identified by the FEMs, but the FEMs made three additional false-positive fracture identifications. These validation results highlight current limitations of these sideways fall impact models specific to the inclusion of an orthopaedic implant. These FEMs present a conservative strategy for fracture prediction in future applications. Further evaluation of the modelling approaches used for the bone-implant interface is recommended for modelling augmented specimens, alongside the importance of maintaining well-controlled experimental conditions.

KEYWORDS

augmentation, biomechanics, falls, finite element models, hip fracture

Emily K. Bliven and Anita Fung contributed equally to this work.

1 | INTRODUCTION

Hip fractures in the elderly are severe injuries and almost always require hospitalisation and surgery.[1] Most geriatric hip fractures are caused by sideways falls[2] and are associated with long-term disability[3] and excess mortality compared to an age-matched population.[4,5] In Europe alone, approximately 610,000 hip fractures were sustained in the year 2010, and this number is expected to increase to 814,000 per year by in the year 2025.[1] Additionally, along with the increased incidence of hip fractures, the associated costs are expected to increase significantly due to an aging population[6] and an increased life expectancy.[1] A mainstay of current hip fracture prevention methods is pharmacological intervention, which demonstrates reduced fracture risk in some populations[7]; however, a meta-analysis has found that these treatments have limited cost-effectiveness in contrast to their high rates of prescription.[8,9] Although hip protectors can attenuate the impact force in sideways falls to some extent, low compliance rates limit their efficacy.[10] However, another study has shown that hip protectors could be cost-effective in long-term care facilities and geriatric wards.[11] Thus, alternative methods for preventing hip fractures have been proposed, such as the use of prophylactic femoral augmentation.[12–14] For example, reinforcing the already-fractured femoral neck has been shown to reduce reoperation risks and rates of secondary fracture.[15] Surgical prophylaxis strategies have also demonstrated cost-effectiveness in elderly patients with high fracture risk.[16]

The aim of prophylactic femoral augmentation is to strengthen a vulnerable femur enough to prevent its fracture in a sideways fall. To this end, various implants[17–20] and bone cement injection patterns[21–27] have been proposed. In these studies, the strength of augmented femurs was measured by loading either the femurs or computational models of the femurs to failure in a standard sideways fall. The loading condition employed in a quasi-static laboratory model used a material test machine.[28,29] One of the major drawbacks of this approach is that the specimens are loaded to the point of fracture regardless of whether the required force to fracture was higher than could plausibly arise from a sideways fall. Another limitation of these approaches is that the quasi-static test setup does not typically represent surrounding tissues such as the pelvis and soft tissue (i.e. skin, muscle, fat) adequately. This omission has a major effect on the results because it has been previously shown that the surrounding tissues absorb up to 95% of the impact energy during a sideways fall.[30–33]

To address these shortcomings, we developed a dynamic inertia-driven sideways fall simulator in our laboratory.[34] The simulator was built to incorporate cadaveric pelvises with both proximal femurs, joint capsules, and surrounding ligaments. The cadaveric specimen is embedded in a soft tissue (ST) surrogate to represent fat, skin, and muscle, and the test setup includes a metal leg assembly of body-appropriate mass that rotates around a foot point to follow an inverted-pendulum motion in the sideways fall. Finite element models (FEMs) of the fall simulator have been developed and validated in past work, showing close agreement for parameters such as peak impact force, effective pelvic stiffness, and fracture production.[35]

Although the validated FEMs of the fall simulator have been subsequently used in an in silico study that examined the prophylactic augmentation effect of different orthopaedic implants, assuming a linear elastic response of the pelvis,[36] the FEMs have not yet been validated (compared for accuracy) with experimental data of this type. The ultimate goal of validating FEMs is to ensure that their use in assessing patient-specific orthopaedic treatments and medical devices is safe, effective, and can improve patient outcomes. To this end, it is essential to quantify the level of agreement between the augmented FEMs and their corresponding experiments to identify potential uncertainties in either model. This furthers their application in providing supporting evidence for clinical development by offering the opportunity for in silico evaluation of interventions over a broader population.[37,38]

Of the three prophylactic augmentation strategies that were evaluated in the previous in silico study,[36] the Gamma3® Trochanteric Nail fracture fixation system (Stryker, Kalamazoo, Michigan, USA) applied with off-label use as a prophylactic was the most effective at increasing the load-bearing capacity of the femurs. Therefore, the aim of this study is to incorporate a reporting checklist[39] to validate the FEMs of specimens augmented with this implant in the sideways fall simulator, by direct comparison with experimental data. To achieve this, impact force measurements, pelvic deformation, effective pelvic stiffness, and fracture outcomes were compared between the ex vivo experiments and the FEMs.

2 | METHODS

2.1 | Fall experiments

Six fresh-frozen post-mortem human specimens (Table 1) containing all tissues between the navel and mid-femur, were acquired from a tissue bank (ScienceCare, Phoenix, AZ, USA). Donors or a next of kin had given written or electronic consent to the donation and institutional ethics approval was gained before experimental work (University of British Columbia Clinical Research Certificate H19-03349).

The methods for specimen dissection and preparation have been previously described.[31]

A fellowship-trained orthopaedic surgeon implanted the left femur of all specimens with a Gamma3® Trochanteric Nail and lag screw using standard clinical protocols and instrumentation under fluoroscopy guidance. Of note, the prophylactic implantation applied in this study is an off-label use of this device. All nails had a neck-shaft angle of 125° and were 180 mm long. Distal reaming diameters and lag screw lengths matched specimen anatomy (Table 2).

Due to concerns of creating stress concentrations on the distal femoral shaft, the distal locking screw was not implanted in any of the specimens. However, preliminary FEM results indicated that the presence of the distal locking screw had a negligible effect on the

TABLE 1 Specimen information. H5050 and H1405 had normal bone density at the left hip, while the other specimens were osteoporotic.

Specimen	H1388	H1393	H1398	H1405	H1407	H5050	Average ± SD
Sex (M/F)	F	F	M	M	F	M	
Age (years)	63	81	83	73	76	81	76 ± 7
Height (m)	1.73	1.52	1.80	1.80	1.73	1.70	1.71 ± 10.2
Body mass (kg)	43.7	61.3	50.8	90	40.4	60.8	57.9 ± 17.9
BMI (kg/m^2)	14.6	26.4	15.7	27.7	13.5	21.0	19.9 ± 6.2
ST on greater trochanter (mm)	11.1	37.0	13.0	31.8	11.5	10.1	19.1 ± 12.0
Hip aBMD (g/cm^2)	0.479	0.462	0.614	0.993	0.416	1.013	0.674 ± 0.269

TABLE 2 Specimen and corresponding distal reaming diameter and length of lag screw.

Specimen	Distal reaming diameter (mm)	Lag screw length (mm)
H1388	12.0	85
H1393	12.0	80
H1398	14.0	105
H1405	15.5	95
H1407	15.5	100
H5050	14.0	85

predicted outcome of the sideways fall. In addition, one study describes that implanting the distal locking screw is not required when fixing stable fractures clinically.[40] The prophylactic application of this implant presents an environment comparable to a stable fracture, which would not warrant the use of the distal locking screw for intramedullary (IM) nailing. The positioning and configuration of the implant was established for each specimen according to this device's recommended surgical technique (for fracture fixation), geometric constraints of the femur, and the surgical expertise of a practicing fellowship-trained trauma surgeon. Exact placement depended on specimen characteristics (such as cortex density and femoral head-shaft angle) but was captured using CT imaging. Device insertion was conducted with the intention to avoid iatrogenic trauma, additional stress concentrations, or any further damage to the femoral structures beyond necessary to achieve implantation.

The soft tissue surrogate preparation, specimen alignment, and fall test were conducted using the same protocol as in the previous study (Figure 1A).[34] Briefly, donated ex vivo human specimens are dissected to the entire pelvis with femurs, leaving joint capsules, cartilage, and ligaments intact. Both femurs are cut to 175 below the greater trochanter and are aligned and embedded with PMMA (polymethyl methyl acrylate) in square tubes that attach to metal leg constructs. Before testing, specimens are cast in a subject-specific mould of 20 weight & ballistic gelatin, the geometry of which is derived from a databased of scanned body sapes and assigned based on sex and BMI. During the fall test, specimens are guided in an inverted pendulum motion before free-falling onto the impact surface. As in previous experiments,[31,34] the impact force of the drop was measured using a modified six-axis force plate (FP4000-15, Bertec Corporation, Columbus, OH, USA) at a sampling frequency of 10,000 Hz. Two high-speed cameras (Phantom v9, Vision Research, Wayne, NJ, USA) were used to track eight pelvis markers and six soft tissue markers (passive spherical markers, 4 mm diameter; CTMark, Suremark®, Simi Valley, CA, USA) during impact at a sampling frequency of 5000 Hz, exposure time of 100 µs, and resolution of 0.3 mm/pixel. The target impact velocity of the fall experiments is 3 m/s,[34] which was established to correspond with real-world fall speeds.[41] The exact fall velocity and directional components for each experiment was calculated using position data from two infra-red-emitting markers on the impacted leg (Optotrak Certus, Northern Digital Inc., Ontario, Canada).

All specimens but two had both femurs cut to 175 mm, which was the length used in our previous study with unaugmented femurs.[31] The left femur of specimens H1393 and H1388 was cut to 215 mm (Figure 1B), as they were potted in PMMA before the decision to omit implantation of the distal locking screw was made. The fall simulator was modified accordingly to accommodate the different lengths for the left femur. This involved shortening the impacting leg thigh piece while keeping the mass, mass moment of inertia, and other structures of the system consistent. These changes were reflected in the corresponding FEMs.

2.2 | FEMs

Clinical-resolution computed tomography (CT) images (scanning protocol: 120 kVp, 200 mAs, voxel size: 0.78 mm × 0.78 mm × 0.3 mm) of the specimens were used to obtain the geometries of each specimen's femurs and pelvis before implantation. CAD models of the nail and lag screw were created using direct measurements made with a caliper. Fine features such as the lag screw threads were not included in the models and this geometry was modelled as a simple cylinder to reduce high computational costs associated with such geometries. The material used for the implant was a titanium model

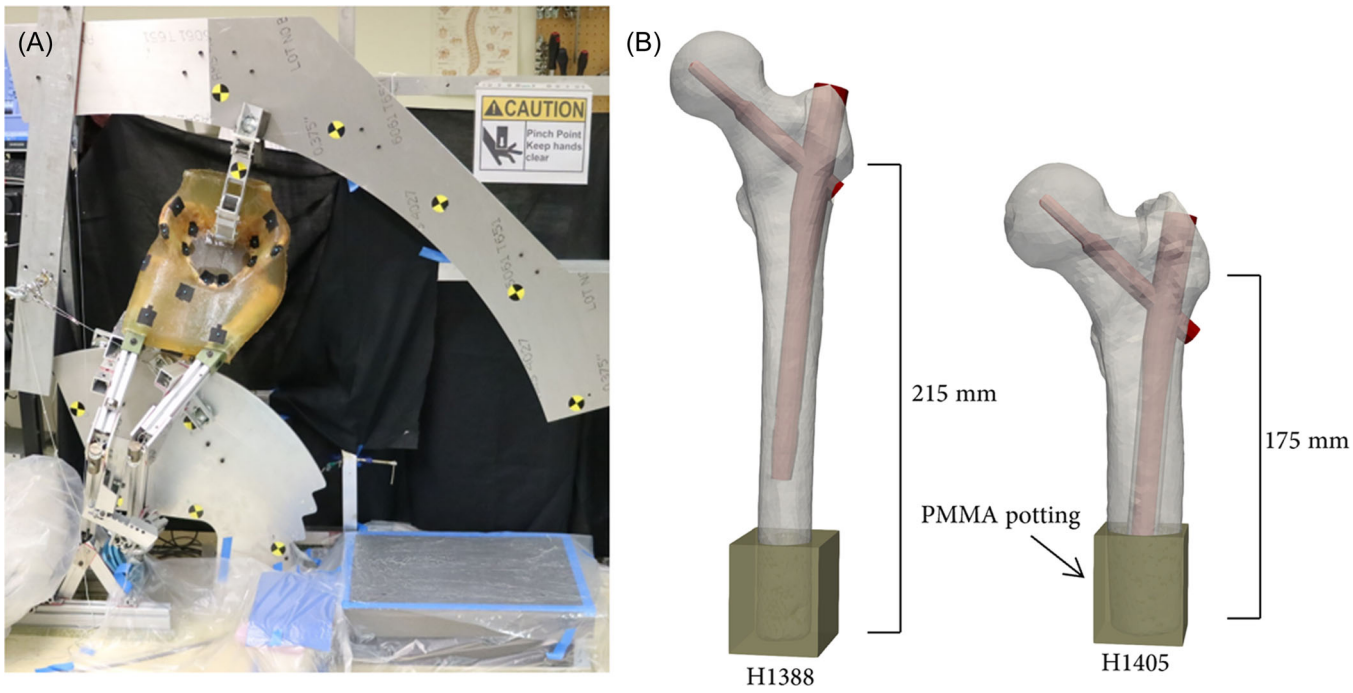

FIGURE 1 (A) Sideways fall simulator and (B) FEM representation of left femur bones and lengths for two specimens augmented by IM nailing.

that was used for the same device in a previous study,[36,42] with a Young's modulus of 110 GPa and a Poisson's ratio of 0.3. An elastic material model (MAT_ELASTIC) was used for the implant as the force magnitudes expected from a standing height fall were not expected to cause plastic deformations in the implant. The masses of the implant models were within 3% of the masses of the physical implants.

The gap between the bone and the distal end of the IM nail was made in accordance with the distal reaming diameters used during implantation (Table 2). The interface between the bone and the lag screw threads was a tied contact. The remainder of the bone-to-implant gaps were made in accordance with methods used in the previous implant FEMs.[36] The contact between the lag screw and IM nail in the FEM was modelled as a tied contact. All other contact pairs between the bone and implant were modelled as frictionless, with the separation and sliding of contacting surfaces allowed. Since the coefficients of friction between the bone and the IM nail and unthreaded section of the lag screw are unknown, may not be constant during the impact, and are difficult to determine, setting these surfaces as frictionless provides a more conservative estimation of the contact behaviour. In real-life scenarios, there would likely be some friction between the bone and the implants, and thus there would be less movement between the surfaces than predicted by the model.

Specimens were also CT scanned postimplantation with the same parameters as above. The implant and left femur from this CT scan were segmented, and segmentation masks were used to determine the positioning of each implant within the femur (Figure 1B). As in the previous FEM study,[36] the nodes on the implant models were aligned along the long axes of the implants to allow for the movement between the implants and also at the bone-implant interface. The material mapping of the augmented femur was conducted using the CT images of the unaugmented femur to avoid error from artifacts caused by the presence of the metal implant in the augmented CT scans. The meshed femur with the implant was then incorporated into the FEM of the rest of the specimen and the fall simulator.

A detailed description of the FEM methodology for unaugmented specimens has been previously published.[30] Similarly to the pelvis and femurs, the implant structures were modelled with tetrahedral elements with an average edge length of 3 mm. Mesh convergence for the impacting femur has been demonstrated in a past study.[43] The mesh size, density-modulus relationships, and material models for bone were assumed to be valid for the present FEMs as well. In this study, the contact at the interface of the soft tissue surrogate and force plate surface (ballistic gel and a plastic sheet coated with KY Jelly) was modelled with a friction coefficient of 0.27, as was measured experimentally using an inclined plate apparatus. The following boundary conditions were assumed to be constant for all experiments: fixed translational degrees of freedom at the foot point of the impacted leg, gravity (9.81 m/s^2) in the global X-direction, and friction neglected for metal-to-metal contact and femoral heads to acetabular cartilage contact.

Simulations with three different material property configurations were run for each specimen. Nonlinear simulations ($FEMs_{non\text{-}lin}$) accounted for yield and post-yield behaviour in the bone tissue,[43] and these fracture outcomes were compared directly to the ex vivo data. Linear simulations ($FEMs_{lin}$), in which the bone materials did not have a yield point,[44] were also run. These simulations were run

in the previous validation study of unaugmented specimens[35] to provide an estimate of the impact kinetics of the subject-specific impacts in the absence of bone failure. The last set of simulations were the elastic pelvis simulations ($FEMs_{ep}$), which had linear elastic properties in the pelvis and nonlinear properties in both femurs. The $FEMs_{ep}$ were run to put the results of the present study in a similar context to previously published studies that used such configurations.[36,37,45]

Per the published reporting checklist[39] for validating FEMs in orthopaedic biomechanics applications, features of the simulation model that have already been presented include: geometry/image acquisition, material properties,[43] element type, mesh density characteristics (edge length), degrees of freedom, contact and boundary conditions, and convergence. Explicit simulations were pre-processed in ANSA software (BETA CAE Systems, Michigan, USA) and solved using LS-DYNA software (Ansys Inc., Pennsylvania, USA) using 12–16 cores on a remote computing platform. Increment size was 0.2 ms timesteps. The coordinate system was defined using digitised points on the surface of the experimental force plate, as in previously published methods.[34] For the validation process, experimental results are provided, put into the context of the literature, and uncertainty quantified in terms of root mean squared error (RMSE) and mean error, as discussed next. The four-eyes principle[39] was achieved through the collaborative nature of this work.

2.3 | Data analysis

Peak impact force (F_{max}), time to peak force (t_{Fmax}), and impulse to peak force (Imp_{Fmax}) were derived for the FEMs from the contact forces between the soft tissue and force plate for comparison to force plate data from the experiments. Fragility ratio (FR) values were calculated as in previous studies[35,36] to quantify the ratio between peak forces in $FEMs_{lin}$ and $FEMs_{non\text{-}lin}$. Previously, FR thresholds of 1.3 and 1.4 were found to differentiate femur from non-femur fracture outcomes for impact surface and femur forces, respectively, for 11 unaugmented specimens.[35] In the experiments, an orthopaedic surgeon (PG) assessed fracture outcomes after post-fall removal of the cadaveric bones from the surrogate soft tissue. In the FEMs, a strain-based criteria using the first and third principal engineering strains (LS-DYNA history variables #18 and #20 for MAT_83) at 2 ms after the peak impact force was used to determine fracture. Strain thresholds for tensile and compressive failure of both trabecular and cortical bone and fracture definition have been described previously (cortical: +0.140, −0.295; trabecular: +0.070, −0.100).[36,46,47] Fracture status was classified as femoral (indicative of hip fracture), pelvic fracture, or non-fracture.

In the ex vivo experiments, the distance between lower ring markers LR1 and LR2 (Figure 2) were tracked over time using the high-speed camera data for each specimen to determine the pelvic compression at 80% of the peak experimental impact force ($C_{LR,F80\%}$). The anatomical placements of LR1 and LR2 were on the lateral ring, directly above the centre of the acetabula.[30,31] In addition, the effective pelvis stiffness (a bulk measurement) in the direction of the fall (k_{sDOF}) was also used as a validation metric.[35] To calculate the k_{sDOF}, the impact force between 500 N and the peak force was plotted against the x-coordinate of the soft tissue marker over the contralateral greater trochanter $d_{ST1,x}$ (Figure 2). The slope of the linear regression of this plot was calculated to be the effective pelvic stiffness, to provide a representation of the stiffness of the system as a whole, similarly to methods used previously.[35,48]

Validation metrics included the RMSE, mean absolute error, and maximum absolute error, which were calculated for parameters F_{max}, t_{Fmax}, Imp_{Fmax}, $C_{LR,F80\%}$, and k_{sDOF}. r^2 values were calculated from the statistically significant linear regressions between each parameter's ex vivo and $FEM_{non\text{-}lin}$ value. RMSE values (Equation 1) for each outcome parameter value (v) were calculated using the below equation for the number of specimens with corresponding data available (n).

$$\mathrm{RMSE} = \sqrt{\frac{\sum(v_{FEM_{non-lin}} - v_{ex\ vivo})^2}{n}} \quad (1)$$

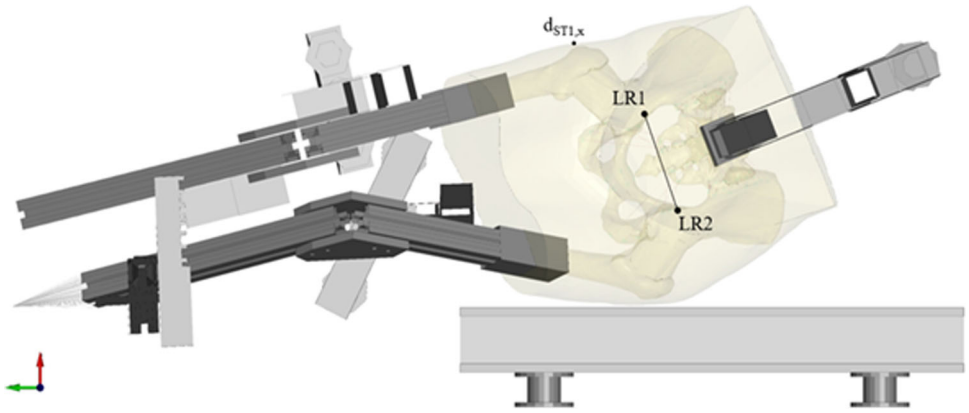

FIGURE 2 FEM of sideways fall simulator. Markers LR1 and LR2 on the pelvic ring represent the markers that were tracked to determine pelvic compression. The marker $d_{ST1,x}$ represents the soft tissue marker over the contralateral greater trochanter.

3 | RESULTS

RMSE values were relatively low (below 15% of the highest corresponding experimental value) for F_{max}, t_{Fmax}, and Imp_{Fmax} (Table 3). $C_{LR,F80\%}$ showed a high RMSE relative to the individually measured experimental values as did k_{sDOF}, with the highest RMSE out of all parameters. The RMSE, mean absolute error, and maximum absolute error of parameters derived from impact force measurements (F_{max}, t_{Fmax}, and Imp_{Fmax}) were all between 11.28% and 24.4% of the maximum respective quantities in the ex vivo experiments. For all specimens, k_{sDOF} was consistently overestimated by the $FEMs_{non\text{-}lin}$ whereas all other parameters varied in being over- or underestimated by the $FEMs_{non\text{-}lin}$ (Figure 3), depending on the specimen. The only significant correlation between $FEMs_{non\text{-}lin}$ and ex vivo data was for t_{Fmax}, with an r^2 value of 0.97.

Comparing the impact forces between the FEMs (Figure 4A), the peak forces were lowest for simulations with failure mechanisms modelled in the femur and pelvis ($FEMs_{non\text{-}lin}$), followed by simulations that only modelled failure in the femur ($FEMs_{ep}$), and highest for simulations that did not model bone failure ($FEMs_{lin}$). In all six specimens, the ex vivo peak forces most closely followed trends for $FEMs_{non\text{-}lin}$. Due to operator error in the experiments, the force trace for H1407 was collected at 1000 Hz and there was no force trace collected for H5050.

C_{LR} had a notably higher magnitude in the ex vivo experiment than in the $FEMs_{non\text{-}lin}$ in H1388 and H1393 (Figure 4B), which are the two specimens exhibiting pelvic fractures in the ex vivo experiments. $C_{LR,F80\%}$ values were relatively similar between all specimens; however, pelvic compression continued to increase well beyond this point in the ex vivo data, and drastically so for H1393 and H1388. When comparing trends between FEMs, the C_{LR} was highest for $FEMs_{non\text{-}lin}$, followed by $FEMs_{lin}$, and lowest for $FEMs_{ep}$. C_{LR} data was unavailable for H1398 after 10.2 ms as the marker was obscured by soft tissue surrogate in the high-speed video data. The $FEMs_{non\text{-}lin}$ consistently underestimated $d_{ST1,x}$ and overestimated k_{sDOF} in comparison to the ex vivo data (Figure 3, Figure 4C). The k_{sDOF} value predicted by $FEMs_{non\text{-}lin}$ was at times close to double (H1388, H1405) or even triple (H1398) the magnitude of the value calculated from experimental ex vivo data.

In the ex vivo experiments, no signs of intertrochanteric or femoral neck fractures were observed in any of the specimens. Specimen H1393 sustained a lateral compression fracture at the left pubic body and ischial ramus, and a 12.5 mm stable fracture on the left pubic ramus was observed in specimen H1388 (Figure 5). For $FEMs_{non\text{-}lin}$, pelvic fracture was accurately predicted in both H1393 and H1388 (true-positives). Similar to findings from ex vivo experiments, no fracture was predicted in H5050 (true-negative). In contrast to the lack of any visible damage found experimentally, $FEMs_{non\text{-}lin}$ predicted three false-positives where strain thresholds were violated: pelvic fractures in H1405 and H1407 and a femoral fracture (isolated greater trochanter) in H1398. The sensitivity and specificity of these $FEMs_{non\text{-}lin}$ for fracture prediction were calculated to be 1.00 and 0.25, respectively.

FR values (Figure 6) did not accurately correspond to predicted fracture status using previously described threshold values for differentiating femoral fracture and non-femoral fracture.[35] Overall, all FR values were below their respective femur fracture thresholds except for H1407 in femur force FR and H1398 in impact force FR. Volumetric strain values of the IM nailing system were below 0.2% (yield for Titanium is approximately 0.5%) indicating that all deformations occurred in the linear range throughout the course of the fall impact.

TABLE 3 Validation metrics for the listed outcome parameters. The values given in parentheses are the corresponding value's percentage of the maximum measured value in the ex vivo data.

	RMSE	Mean absolute error	Maximum absolute error
F_{max} (kN)	0.761 (13.4%)	0.64 (11.2%)	1.26 (22.2%)
t_{Fmax} (ms)	0.54 (13.9%)	2.36 (12.8%)	3.89 (21.0%)
Imp_{Fmax} (Ns)	13.8 (14.5%)	11.3 (11.8%)	23.3 (24.4%)
$C_{LR,F80\%}$ (mm)	1.34 (39.7%)	0.46 (33.2%)	0.99 (72.4%)
k_{sDOF} (N/mm)	140 (68.6%)	121.2 (59.4%)	192.6 (94.4%)

4 | DISCUSSION

The aim of this study was to use ex vivo data to validate the FEMs of corresponding specimens augmented by prophylactic IM nailing in a sideways fall simulator. Force-derived parameters (F_{max}, t_{Fmax}, and Imp_{Fmax}) showed moderate to good prediction accuracy between the ex vivo experiments and the $FEMs_{non\text{-}lin}$ in terms of RMSE. Experimental values for $C_{LR,F80\%}$ were not accurately predicted by

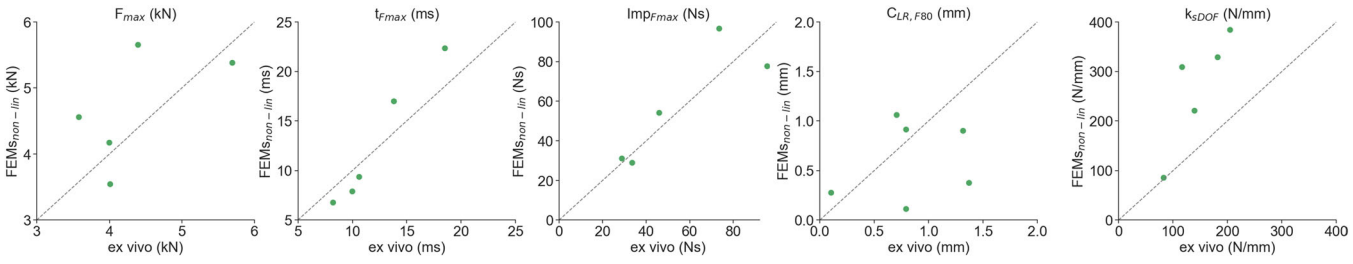

FIGURE 3 Outcome parameters predicted by the $FEMs_{non\text{-}lin}$ vs. experimental ex vivo data.

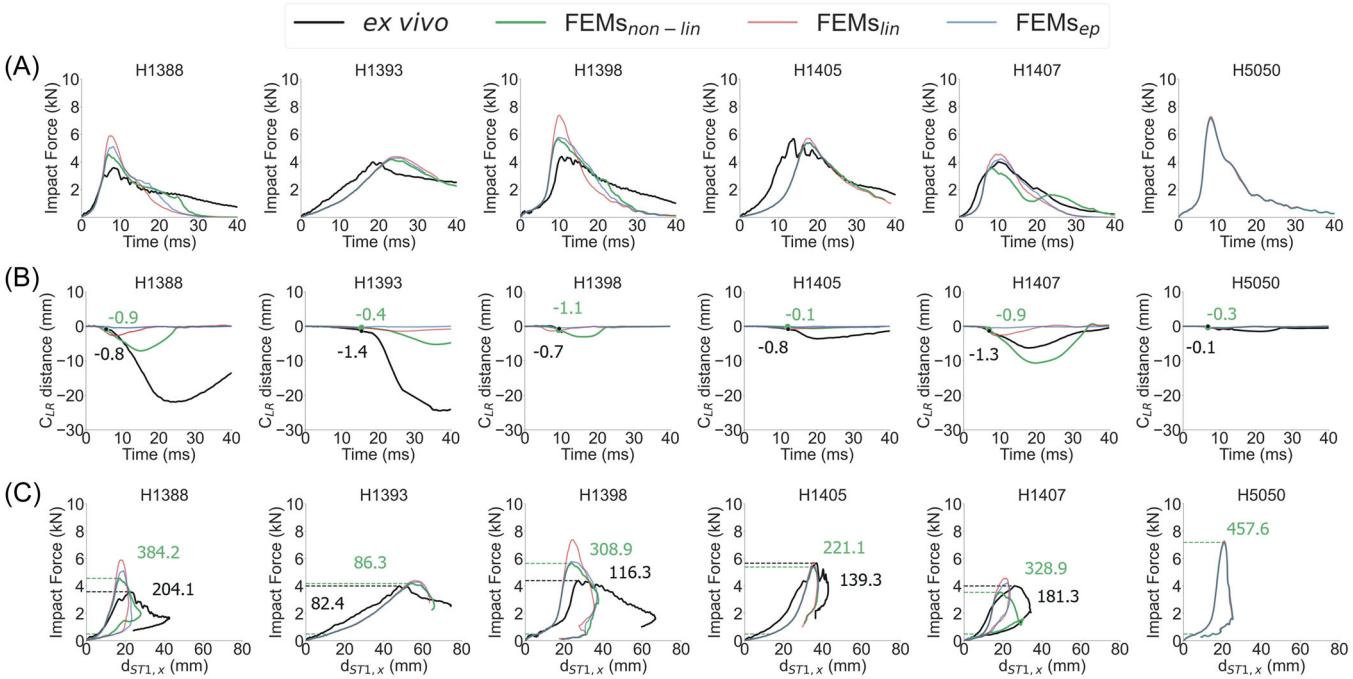

FIGURE 4 Plots show the following outcomes for each specimen from ex vivo experimental data and all FEM configurations: (A) Surface impact forces; (B) Distance between lower ring markers (pelvic compression, C_{LR}). Plotted marker labels denote $C_{LR,F80\%}$ values (mm) for ex vivo and $FEMs_{non\text{-}lin}$ data; (C) Contralateral greater trochanter soft tissue deflection in the direction of the fall ($d_{ST1,x}$) plotted against surface impact force. Labelled values denote the k_{sDOF} value (N/mm) for ex vivo and $FEMs_{non\text{-}lin}$, and the dashed horizontal lines indicate the region for which it was calculated (500 N – peak force).

$FEMs_{non\text{-}lin}$ and k_{sDOF} was consistently overestimated by our models. However, the mean absolute error for $C_{LR,F80\%}$ was 0.46 mm, which is similar in magnitude to both the resolution of our cameras and the reconstruction error associated with this method.[34] Differences in $C_{LR,F80\%}$ between $FEMs_{non\text{-}lin}$ and the experiments for H1398, H1405, and H5050 were within the magnitude of this error. The $FEMs_{non\text{-}lin}$ could accurately predict fracture status in four out of six specimens, with no false-negative fracture identifications.

The overestimated k_{sDOF} in our FEMs indicates that the specimen in the FEM is behaving more stiffly than the ex vivo experiments. Assuming an impact without failure of any structures, it would then follow that the F_{max} is also overestimated or that t_{Fmax} is underestimated, causing the strains in the bone to be higher in magnitude or occur over a shorter timespan. This corresponds to the FEM prediction of a femoral and pelvic fracture in H1398 and H1407, respectively, which are both false-positive identifications. Although there was no visual observation of gross damage in the form of displaced fracture fragments found for these specimens ex vivo, it may be that there is plastic damage or other permanent deformation of the bone structures at the locations predicted by the FEM (potentially internal damage limited to the cancellous bone without cortical failure seen on visual inspection or CT). In contrast, an enhanced modelling method for the cortical shell at the surfaces of the femur and pelvis may not predict high surfaces strains in the FEMs (as is occurring in the false positive identifications), and better correspond with visual observation of the ex vivo bone surfaces.

For fracture prediction, our $FEMs_{non\text{-}lin}$ showed a high sensitivity for fracture prediction and a lower specificity of 0.25; of note, both values should be interpreted with caution due to the low sample size of this study. Despite the three apparent false-positive identifications, all fractures that were found experimentally were identified and correctly classified by $FEMs_{non\text{-}lin}$. Although three non-fractures were incorrectly classified as fractures (two in the pelvis and one in the femur), this method provides a conservative model that can offer insights for making relative comparisons between interventions. In this study, FR values for specimens without fractures and with pelvic fractures were overlapping (Figure 6), which is in agreement with past applications of this metric.[35]

When comparing to a past validation of these FEMs conducted for unaugmented native pelvis-femur specimens,[35] the RMSE values found here were generally higher on a scale of 2–4 times. This reduction in accuracy when modelling augmented femurs may be due to inaccuracies in the modelling of the Gamma Nail implant, the bone-implant interface, or inaccuracies associated with running the ex vivo experiments. There was moderate tearing of the soft tissue surrogate gel in H1398 that resulted in the partial loss of C_{LR} data and may have led to experimental-FEM inconsistencies as these tears were not modelled in silico. However, other specimens with mild to moderate gel tearing (H1393, H1405) showed better agreement in validation outcomes, suggesting that, overall, effects of gel discontinuity may be negligible for some parameters up until the time of peak force. This would be because tearing in H1398 was present before test initiation, whereas for H1393 and H1405, gel tearing did not appear to

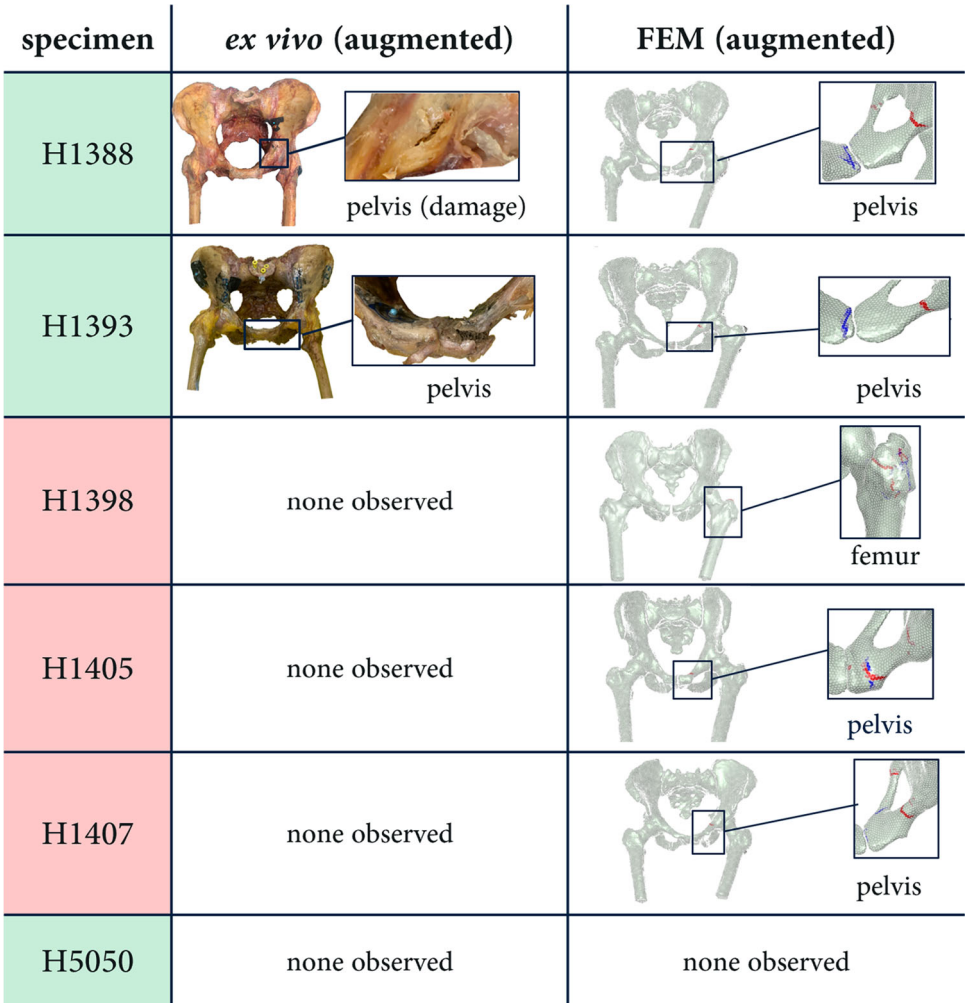

FIGURE 5 Fracture outcomes from ex vivo experiments and $FEMs_{non\text{-}lin}$. Red and blue colours in the right column denote elements whose strain values exceeded thresholds for tension and compression respectively. Green specimen shading indicates a true-negative or true-positive classification by the FEM and red specimen shading indicates a false-positive classification.

become more severe until after peak force, as confirmed by high-speed video. It is likely that the outcome parameter most affected by a potential loss of rigid contact between the bone and soft tissue (from gel tearing) is $k_{sDOF,}$ which is reflected in the corresponding high RMSE values.

With respect to the higher stiffnesses observed in our FEMs compared to experimental values, it may be that a fully bonded contact at the interface of the screw threads and bone does not adequately represent the ex vivo situation. This would be particularly relevant for osteoporotic patients, where achieving sufficient orthopaedic screw purchase is generally less successful due to the increased porosity in the trabecular bone,[49] lowering local stiffnesses. Gap size between the implant and adjacent bone may change in the clinical scenario due to repositioning from surgical error, which is a valid concern when it comes to prophylactic augmentation.[50] A combination of larger-than-modelled bone-implant spacing and the presence of porous bone adjacent to the implant may have contributed to a higher stiffness in our FEMs than observed experimentally; particularly because the material model used for bone in the FEMs is a foam material with no representation of empty space.

Other approaches found in the literature for validating FEMs of specimens with prophylactic augmentation are limited to work with cement injections, reporting error in yield load predictions of 15.6%[51] and 20.3%,[26] which are higher than but comparable to our value of 11.2% error for peak impact force. Other attempts to validate bone with implanted hardware extend to quasi-static loading of hemi pelvises,[52] total knee arthroplasties,[53] or hip arthroplasty stems in the femur.[54] Results of these studies generally showed high accuracies but tested bone-only specimens without adequate representation of soft tissue structures, or application of inertial loading. Our application of the fall simulator adds complexity to the method (and likely variability to our results), but both of these aspects are paramount to produce a representation of injurious loading that has improved biofidelity with the in vivo situation.[55,56]

As in all ex vivo and FEM studies, this study has some limitations. Although useful for visualising agreement, r^2 as a metric has long-demonstrated limitations to its application in terms of precisely

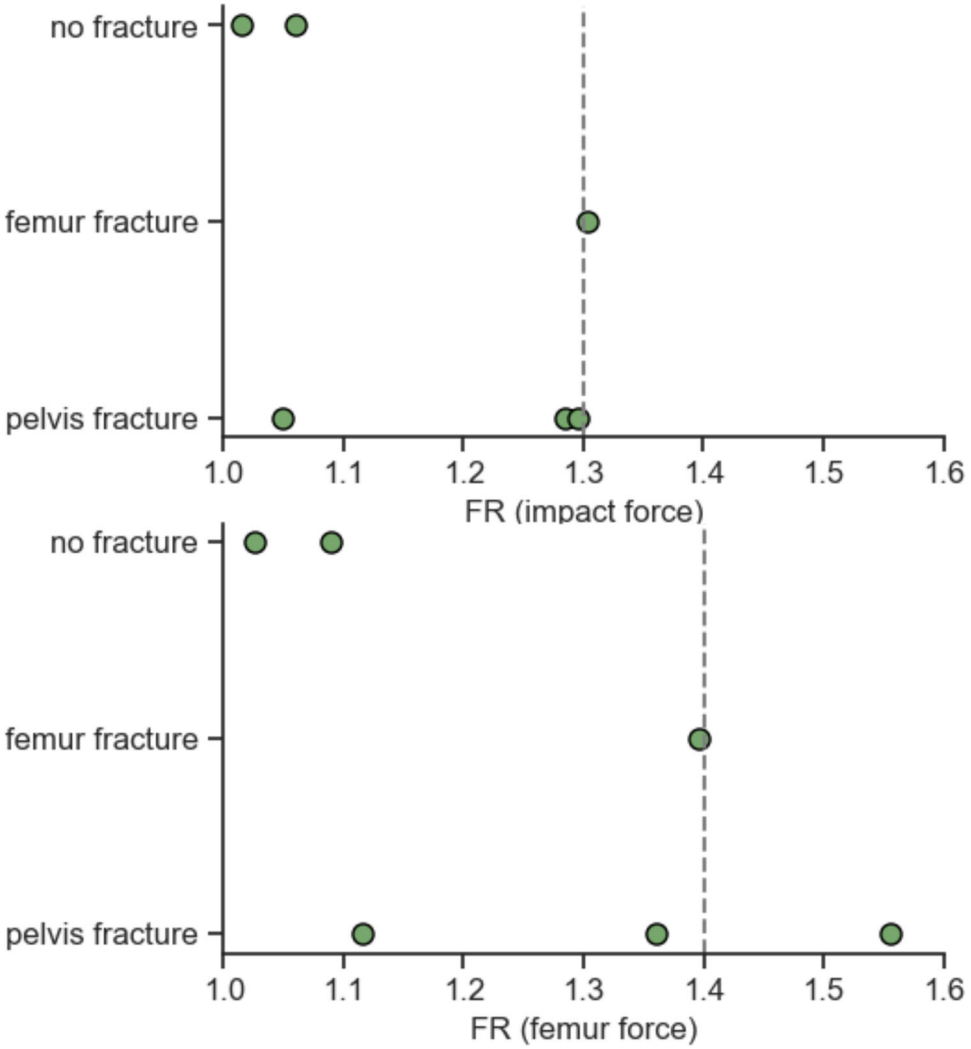

FIGURE 6 FR values calculated using surface impact force and femur force. Fracture outcomes provided are those predicted by $FEMs_{non\text{-}lin}$. The dashed vertical line indicates previously described thresholds for differentiating between femoral fracture and non-femoral fracture.[32]

representing correlations[57] and, due to the small sample size used here, should be interpreted with caution in its implications for t_{Fmax}. It was discovered that the digitisation probe used to characterise the initial positioning of the specimen and fall simulator was improperly calibrated for specimens H1393 and H1388. Although this mis-calibration was corrected for to the extent possible, it may have contributed to the lack of agreement between the experiments and FEMs in these tests. The relatively large femur element size does not allow our model to capture the potential presence of stress concentrations around the implant. The relatively small number of specimens tested makes it difficult to draw definitive conclusions from the results. Limitations of the fall simulator have been outlined in a previous study,[31] some of which include the absence of muscle activation and subject-specific soft tissue properties, the effect of the upper body, and the lack of compliance in the leg constructs. Finally, despite it being the most relevant scenario for hip fracture in the elderly,[58] only one fall alignment and impact velocity were applied in this study.

The context of use for this model was to generate a basic understanding of hip fracture mechanics and prevention. It is low risk, as no application to clinical practice is directly targeted, but the model has high influence, as it would likely be used without further experimental testing. The outcome of this validation is a comparison to experimental values with mixed results. Further model development and validation would be needed to establish increased model credibility.

5 | CONCLUSION

This study compared the impact response and fracture outcomes of ex vivo cadaveric specimens with femurs augmented by IM nailing in a sideways fall with corresponding FEM predictions. Compared to previous FEM studies of unaugmented specimens tested using the sideways fall simulator, the presented $FEMs_{non\text{-}lin}$ tended to over-predict effective pelvic stiffness and showed higher variability in accurately reporting experimental F_{max} and C_{LR} values. However, $FEMs_{non\text{-}lin}$ demonstrated moderate accuracy at predicting t_{Fmax}, Imp_{Fmax}, and k_{sDOF} when a fracture fixation device was used to prophylactically augment the femur. No femoral fractures were

observed for the six ex vivo tests, and the trend for a false-positive identification of fracture in the $FEMs_{non\text{-}lin}$ supports the use of similar models to provide conservative estimates when comparing interventions in other studies. Overall, these results suggest that these FEMs are a reasonable approach for predicting fall experiment outcomes of augmented specimens, but demonstrate variations possibly linked to repeatability issues with running the ex vivo experiments or accurately representing the orthopaedic implant component within bone in the FEMs. Maintaining well-controlled experimental conditions (i.e., the soft tissue shape) is of priority in future testing. The further development of various aspects of modelling approaches, particularly concerning modelling of the bone-implant interface under loading, should be considered to improve the overall accuracy of the FEMs for modelling fall scenarios with augmented specimens.

AUTHOR CONTRIBUTIONS

All authors have read and approved the final submitted manuscript. The authors confirm contribution to the paper as follows: study conception and design: A Fung, I Fleps, SJ Ferguson, B Helgason; data collection: EK Bliven, A Fung; analysis and interpretation of results; EK Bliven, A Fung, A Baker, I Fleps, SJ Ferguson, B Helgason, PA Cripton; draft manuscript preparation: EK Bliven, A Fung, I Fleps, P Guy, B Helgason, PA Cripton.

ACKNOWLEDGMENTS

This project was funded by the Swiss National Science Foundation (Grant no. 205320_169331), grants #2018-430 and #2018-430 of the Strategic Focus Area "Personalised Health and Related Technologies" of the ETH Domain, ETH Zurich, Switzerland, and the Friedman Award for Scholars in Health from the University of British Columbia. The authors are grateful for the implant donations provided by Stryker in this project. The authors would also like to thank Jennifer Powell and Vivian Arnst in the Vancouver General Hospital Radiology Department for their help and expertise with collecting the CT data instrumental to this study. Also, many thanks to Jade Levine and Sophia Katramadakis for their invaluable assistance in conducting the fall experiments.

ORCID

Emily K. Bliven http://orcid.org/0000-0002-7376-5886

REFERENCES

1. Hernlund E, Svedbom A, Ivergård M, et al. Osteoporosis in the european union: medical management, epidemiology and economic burden: a report prepared in collaboration with the international osteoporosis foundation (IOF) and the european federation of pharmaceutical industry associations (EFPIA). *Arch Osteoporos*. 2013;8(1-2):136.
2. Parkkari J, Kannus P, Palvanen M, et al. Majority of hip fractures occur as a result of a fall and impact on the greater trochanter of the femur: a prospective controlled hip fracture study with 206 consecutive patients. *Calcif Tissue Int*. 1999;65(3):183-187.
3. Marottoli RA, Berkman LF, Cooney LM. Decline in physical function following hip fracture. *J Am Geriatr Soc*. 1992;40(9):861-866.
4. Abrahamsen B, Van Staa T, Ariely R, Olson M, Cooper C. Excess mortality following hip fracture: a systematic epidemiological review. *Osteoporos Int*. 2009;20(10):1633-1650.
5. Liow MHL, Ganesan G, Chen JDY, et al. Excess mortality after hip fracture: fracture or pre-fall comorbidity? *Osteoporos Int*. 2021;32(12):2485-2492.
6. Papadimitropoulos EA, Coyte PC, Josse RG, Greenwood CE. Current and projected rates of hip fracture in Canada. *CMAJ*. 1997;157(10):1357-1363.
7. Papapoulos SE, Quandt SA, Liberman UA, Hochberg MC, Thompson DE. Meta-analysis of the efficacy of alendronate for the prevention of hip fractures in postmenopausal women. *Osteoporos Int*. 2005;16(5):468-474.
8. Järvinen TLN, Michaëlsson K, Jokihaara J, et al. Overdiagnosis of bone fragility in the quest to prevent hip fracture. *BMJ*. 2015;350(May):h2088.
9. Initiative Therapeutics. A systematic review on the efficacy of bisphosphonates. 2011;(83):1-2.
10. Body JJ, Bergmann P, Boonen S, et al. Non-pharmacological management of osteoporosis: a consensus of the Belgian bone club. *Osteoporos Int*. 2011;22(11):2769-2788.
11. De Bot RTAL, Veldman HD, Witlox AM, van Rhijn LW, Hiligsmann M. Hip protectors are cost-effective in the prevention of hip fractures in patients with high fracture risk. *Osteoporos Int*. 2020;31(7):1217-1229.
12. Howe JG, Hill RS, Stroncek JD, et al. Treatment of bone loss in proximal femurs of postmenopausal osteoporotic women with AGN1 local osteo-enhancement procedure (LOEP) increases hip bone mineral density and hip strength: a long-term prospective cohort study. *Osteopor Int*. 2019;31(5):921-929.
13. Cornelis FH, Tselikas L, Carteret T, et al. A novel implant for the prophylactic treatment of impending pathological fractures of the proximal femur: results from a prospective, First-in-Man study. *Cardiovasc Intervent Radiol*. 2017;40(7):1070-1076.
14. Rodrigues L, Cornelis FH, Chevret S. Hip fracture prevention in osteoporotic elderly and cancer patients: an on-line French survey evaluating current needs. *Medicina*. 2020;56(8):397.
15. Bögl HP, Zdolsek G, Michaëlsson K, Höijer J, Schilcher J. Reduced risk of reoperation using intramedullary nailing with femoral neck protection in Low-Energy femoral shaft fractures. *J Bone Jt Surg*. 2020;102(17):1486-1494.
16. Alnemer MS, Kotliar KE, Neuhaus V, Pape HC, Ciritsis BD. Cost-effectiveness analysis of surgical proximal femur fracture prevention in elderly: a Markov cohort simulation model. *Cost Effectiv Resour Allocat*. 2023;21(1):77.
17. Szpalski M, Gunzburg R, Aebi M, et al. A new approach to prevent contralateral hip fracture: evaluation of the effectiveness of a fracture preventing implant. *Clin Biomech*. 2015;30(7):713-719.
18. Springorum HR, Gebauer M, Mehrl A, et al. Fracture prevention by prophylactic femoroplasty of the proximal femur - metallic compared with cemented augmentation. *J Orthop Trauma*. 2014;28(7):403-409.
19. Giannini S, Chiarello E, Mazzotti A, Tedesco G, Faldini C. Surgical prevention of femoral neck fractures in elderly osteoporotic patients: a randomised controlled study on the prevention nail system device. *HIP Int*. 2018;28(25):78-83.
20. Raas C, Hofmann-Fliri L, Hörmann R, Schmoelz W. Prophylactic augmentation of the proximal femur: an investigation of two techniques. *Arch Orthop Trauma Surg*. 2016;136(3):345-351.
21. Heini PF, Franz T, Fankhauser C, Gasser B, Ganz R. Femoroplasty-augmentation of mechanical properties in the osteoporotic proximal femur: a biomechanical investigation of PMMA reinforcement in cadaver bones. *Clin Biomech*. 2004;19(5):506-512.
22. Sutter EG, Mears SC, Belkoff SM. A biomechanical evaluation of femoroplasty under simulated fall conditions. *J Orthop Trauma*. 2010;24(2):95-99.
23. Beckmann J, Ferguson SJ, Gebauer M, Luering C, Gasser B, Heini P. Femoroplasty - augmentation of the proximal femur with a composite bone cement - feasibility, biomechanical properties and osteosynthesis potential. *Med Eng Phys*. 2007;29(7):755-764.

24. Stroncek JD, Shaul JL, Favell D, et al. In vitro injection of osteoporotic cadaveric femurs with a triphasic calcium-based implant confers immediate biomechanical integrity. *J Orthop Res*. 2019;37(4):908-915.
25. Sutter EG, Wall SJ, Mears SC, Belkoff SM. The effect of cement placement on augmentation of the osteoporotic proximal femur. *Geriatr Orthop Surg Rehabil*. 2010;1(1):22-26.
26. Basafa E, Murphy RJ, Otake Y, et al. Subject-specific planning of femoroplasty: an experimental verification study. *J Biomech*. 2015;48(1):59-64.
27. Beckmann J, Springorum R, Vettorazzi E, et al. Fracture prevention by femoroplasty-cement augmentation of the proximal femur. *J Orthop Res*. 2011;29(11):1753-1758.
28. Courtney AC, Wachtel EF, Myers ER, Hayes WC. Effects of loading rate on strength of the proximal femur. *Calcif Tissue Int*. 1994;55(1):53-58.
29. Johannesdottir F, Thrall E, Muller J, Keaveny TM, Kopperdahl DL, Bouxsein ML. Comparison of non-invasive assessments of strength of the proximal femur. *Bone*. 2017;105:93-102.
30. Fleps I, Enns-Bray WS, Guy P, Ferguson SJ, Cripton PA, Helgason B. On the internal reaction forces, energy absorption, and fracture in the hip during simulated sideways fall impact. *PLoS ONE*. 2018;13(8):e0200952.
31. Fleps I, Fung A, Guy P, Ferguson SJ, Helgason B, Cripton PA. Subject-specific ex vivo simulations for hip fracture risk assessment in sideways falls. *Bone*. 2019;125:36-45.
32. Laing AC, Robinovitch SN. Characterizing the effective stiffness of the pelvis during sideways falls on the hip. *J Biomech*. 2010;43(10):1898-1904.
33. Robinovitch SN, McMahon TA, Hayes WC. Force attenuation in trochanteric soft tissues during impact from a fall. *J Orthop Res*. 1995;13(6):956-962.
34. Fleps I, Vuille M, Melnyk A, et al. A novel sideways fall simulator to study hip fractures ex vivo. *PLoS ONE*. 2018;13(7):e0201096.
35. Fleps I, Guy P, Ferguson SJ, Cripton PA, Helgason B. Explicit finite element models accurately predict subject-specific and velocity-dependent kinetics of sideways fall impact. *J Bone Miner Res*. 2019;34(10):1837-1850.
36. Fung A, Fleps I, Cripton PA, Guy P, Ferguson SJ, Helgason B. Prophylactic augmentation implants in the proximal femur for hip fracture prevention: an in silico investigation of simulated sideways fall impacts. *J Mech Behav Biomed Mater*. 2022;126(February 2022):104957.
37. Enns-Bray WS, Bahaloo H, Fleps I, et al. Biofidelic finite element models for accurately classifying hip fracture in a retrospective clinical study of elderly women from the AGES Reykjavik cohort. *Bone*. 2019;120(March 2018):25-37.
38. Viceconti M, Pappalardo F, Rodriguez B, Horner M, Bischoff J, Musuamba Tshinanu F. In silico trials: verification, validation and uncertainty quantification of predictive models used in the regulatory evaluation of biomedical products. *Methods*. 2021;185(November 2019):120-127.
39. Oefner C, Herrmann S, Kebbach M, Lange HE, Kluess D, Woiczinski M. Reporting checklist for verification and validation of finite element analysis in orthopedic and trauma biomechanics. *Med Eng Phys*. 2021;92:25-32.
40. Buruian A, Silva Gomes F, Roseiro T, et al. Distal interlocking for short trochanteric nails: static, dynamic or no locking? Review of the literature and decision algorithm. *EFORT Open Rev*. 2020;5(7):421-429.
41. van den Kroonenberg AJ, Hayes WC, McMahon TA. Hip impact velocities and body configurations for voluntary falls from standing height. *J Biomech*. 1996;29(6):807-811.
42. Niinomi M. Mechanical properties of biomedical titanium alloys. *Mater Sci Eng A*. 1998;243(1-2):231-236.
43. Enns-Bray WS, Bahaloo H, Fleps I, et al. Material mapping strategy to improve the predicted response of the proximal femur to a sideways fall impact. *J Mech Behav Biomed Mater*. 2018;78(August 2016):196-205.
44. Fleps I, Pálsson H, Baker A, et al. Finite element derived femoral strength is a better predictor of hip fracture risk than aBMD in the AGES Reykjavik study cohort. *Bone*. 2022;154:116219.
45. Fung A, Fleps I, Cripton PA, Guy P, Ferguson SJ, Helgason B. The efficacy of femoral augmentation for hip fracture prevention using ceramic-based cements: a preliminary experimentally-driven finite element investigation. *Front Bioeng Biotechnol*. 2023;11(January):1-13.
46. Grassi L, Fleps I, Sahlstedt H, et al. Validation of 3D finite element models from simulated DXA images for biofidelic simulations of sideways fall impact to the hip. *Bone*. 2021;142(October 2020):115678.
47. Galliker ES, Laing AC, Ferguson SJ, Helgason B, Fleps I. The influence of fall direction and hip protector on fracture risk: FE model predictions driven by experimental data. *Ann Biomed Eng*. 2022;50(3):278-290.
48. Robinovitch SN, Hayes WC, McMahon TA. Prediction of femoral impact forces in falls on the hip. *J Biomech Eng*. 1991;113(4):366-374.
49. Ramaswamy R, Evans S, Kosashvili Y. Holding power of variable pitch screws in osteoporotic, osteopenic and normal bone: are all screws created equal. *Injury*. 2010;41(2):179-183.
50. Varga P, Hofmann-Fliri L, Blauth M, Windolf M. Prophylactic augmentation of the osteoporotic proximal femur—mission impossible. *Bonekey Rep*. 2016;5:854 [cited 2020 Feb 2] Available from: http://www.portico.org/Portico/article?article=phx24t34575
51. Basafa E, Armiger RS, Kutzer MD, Belkoff SM, Mears SC, Armand M. Patient-specific finite element modeling for femoral bone augmentation. *Med Eng Phys*. 2013;35(6):860-865.
52. Kluess D, Souffrant R, Mittelmeier W, Wree A, Schmitz KP, Bader R. A convenient approach for finite-element-analyses of orthopaedic implants in bone contact: modeling and experimental validation. *Comput Methods Programs Biomed*. 2009;95(1):23-30.
53. Woiczinski M, Steinbrück A, Weber P, Müller PE, Jansson V, Schröder C. Development and validation of a weight-bearing finite element model for total knee replacement. *Comput Methods Biomech Biomed Engin*. 2016;19(10):1033-1045.
54. Katz Y, Lubovsky O, Yosibash Z. Patient-specific finite element analysis of femurs with cemented hip implants. *Clin Biomech*. 2018;58:74-89.
55. Bouxsein ML, Szulc P, Munoz F, Thrall E, Sornay-Rendu E, Delmas PD. Contribution of trochanteric soft tissues to fall force estimates, the factor of risk, and prediction of hip fracture risk. *J Bone Miner Res*. 2007;22(6):825-831.
56. Gilchrist S, Guy P, Cripton PA. Development of an Inertia-Driven model of sideways fall for detailed study of femur fracture mechanics. *J Biomech Eng*. 2013;135(12):121001121001.
57. Barrett JP. The coefficient of determination—some limitations. *Am Stat*. 1974;28(1):19-20.
58. Kannus P, Leiponen P, Parkkari J, Palvanen M, Järvinen M. A sideways fall and hip fracture. *Bone*. 2006;39(2):383-384.

How to cite this article: Bliven EK, Fung A, Baker A, et al. How accurately do finite element models predict the fall impact response of ex vivo specimens augmented by prophylactic intramedullary nailing? *J Orthop Res*. 2025;43:396-406. doi:10.1002/jor.25984